J. Hydrol. Hydromech., 74, 2026, 2, 84–97
https://doi.org/10.2478/johh-2026-0007

Journal of Hydrology and Hydromechanics

Backward analysis of the Bílá Desná dam break outflow

Jaromír Říha* and Stanislav Kotaška

Brno University of Technology, Faculty of Civil Engineering, Institute of Water Structures, Veveří 331/95, 602 00 Brno, Czech Republic.
* Corresponding author. E-mail: riha.j@vutbr.cz

Abstract: In September 1916, the Austro-Hungarian Empire (today the Czech Republic) experienced the failure of the embankment dam Bílá Desná (historically named Weiße Desse), which at that time was the most disastrous dam failure in central Europe. In this study, available information on the failure of the Bílá Desná dam was gathered and analysed. The initiating cause of the Bílá Desná dam failure was an internal erosion. For the backward analysis of the dam failure, the method of analogy, empirical formulae, and three numerical models, AREBA, DL Breach and HEC-RAS were used. Due to uncertainty in the reservoir volume, the solution was carried out for the originally determined (during the dam design) and newly determined reservoir volumes. The analysis indicates the peak breach outflow range between about 360 and 810 m^3/s. The most realistic and probable peak outflow discharge is about 520 m^3/s. The comparison of individual methods indicate that the AREBA numerical model using Opendata (2024) provides the most realistic failure hydrograph.

Keywords: Bílá Desná; Dam; Breach; Internal erosion; Backward analysis.

1 INTRODUCTION

Dam break studies are of significant interest to civil engineers worldwide. Reconstructing historical dam failure events through backward analysis is crucial for improving our understanding of the mechanisms of initiation and progression of the breach. Although predictive models have advanced significantly and have been calibrated by overtopping or piping scenarios from recent cases, numerous dam failures in the past have not been adequately explored and analysed using modern methodologies. The Bílá Desná dam breach, a seminal incident in the history of dam safety in central Europe, exemplifies this knowledge gap. In many cases, original records lack of the detailed hydrological and breach hydrograph information (Aureli, 2021), which may complicate more accurate modelling and risk assessment today.

Dam breach modelling has been developed since the late 1960s of the last century. Based on the historical failures of embankment dams up to 1965, Cristofano (1973) simulated the onset of soil erosion on the dam surface. In the early 1980s, the BRDAM model (Brown and Rogers, 1981) was developed to simulate the overtopping and internal erosion processes. Nogueira (1988) presented a one-dimensional (1D) model using the Saint-Venant equations to describe unsteady flow, completed by the Exner, Meyer-Peter and Müller equations for sediment transport. Fread (1984, 1988a, 1988b) introduced a set of numerical simulation models for dam break, namely BREACH and DAMBRK, which allowed simulation of a dam breach via both overtopping and internal erosion, including the effects of lateral slope collapses due to sliding. Models were based on complex 1D hydrodynamics and erosion processes, considering soil strength characteristics. An improved BEED model (Singh and Scarlatos, 1988) also simulated erosion processes during dam breaching. Wahl (1998) summarized empirical and numerical procedures, which recommended further improvement of the numerical models. These works were followed by Říha and Daněček (2000) and Tingsanchali and Chinnarasri (2001), while others used different approaches to derive a breach outflow hydrograph using analytical solutions and simulation procedures.

Later, HR Wallingford staff (Mohamed et al., 2002; Morris, 2011; Davison et al., 2013) proposed the HR BREACH model, transformed into the Embankment Breach EMBREA code. The software enables input intervals to characterize soil properties and performs Monte Carlo simulations to find the most unfavourable results. Over the years, other codes have been introduced, such as WOLF, SIMBA and WINDAM, MIKE11 DB (Dewals et al., 2002; Hanson et al., 2005; DHI, 2003). The code Breach_Macchione was incorporated into the software Basement by Voltz et al. (2012).

In 2012, van Damme et al. (2012) A Rapid Embankment Breach Assessment (AREBA) software. After 2014, AREBA was transferred to a user-friendly environment. The code can simulate a dam break due to overtopping and/or internal erosion/piping in homogeneous and zoned embankments. AREBA calculates the breaching process in a very short time, allowing the user to apply an uncertainty analysis. The most valuable feature was that the code was validated using field data. Finally, the AREBA code was modified as part of the project (BMVP, 2025).

Numerous backward studies have been published during the last few decades. For example, Jarret and Costa (1986) developed a backward dam-break model of Lawn Lake Dam and Cascade Lake Dam Failures. Jun and Oh (1998) modelled the Yeonchun Dam Failure using the DAMBRK model and downstream dam-break flood analysis in HEC-1. Risher et al. (2017) validated the Levee Breach Consequence Model through a case study in Joso, Japan, using HEC-RAS. Zhong et al. (2020) conducted a backward analysis of the breaching process of the Baige landslide dam. They used a numerical method based on hydrodynamics, soil erosion, and breach development. These modules were programmed using an iterative method in Microsoft Excel. Lumbroso et al. (2021) modelled the failure of the Brumadinho tailings dam in Brazil in 2019. Petškovek et al. (2021) conducted a backward analysis of the Mount Polley and

Merriespruit dam failures using the EMBREA-MUD dam-breach model, which is suitable for tailings dams.

Numerous studies focused on numerical solution of dam break flow over erodible bed (Khoshkonesh et al., 2024), dam break wave propagation to the area downstream of the dam (Oguzhan and Aksoy, 2020; Rahou and Korichi, 2023) and other related issues.

Previous studies aimed to estimate the peak discharge during the Bílá Desná breach. They have reported a wide range of peak discharge values, reflecting differences in methods, assumptions, and data sources. Raška and Emmer (2014) estimated peak discharges ranging from approximately 418 to 972 m³/s based on detailed geomorphological reconstructions. Froehlich (2016), Azimi et al. (2017) and Moglen et al. (2019) suggested a lower peak discharge close to 320 m³/s using empirical and numerical models. Bernard-Garcia and Mahdi (2019) presented a range between 320 and 656 m³/s based on a comprehensive database of dam failures. More recently, Abdulrahman (2022) estimated the peak discharge to be approximately 591 m³/s using HydroCAD; however, details on input parameters were not fully disclosed. This variability reflects the uncertainties inherent in reconstructing historical dam breaches, primarily due to limited and inconsistent data. It emphasizes the importance of integrating diverse modelling approaches and data sources to reduce uncertainty and improve confidence in peak discharge estimates.

Factual information and data on the Bílá Desná dam failure are summarized and analysed in the preceding study (Kotaška and Říha, 2025).

This study applies state-of-the-art breach modelling techniques and systematically reconstructs and critically evaluates the failure of the Bílá Desná dam in 1916. A multiple criteria comparative framework was adopted, which incorporated the analogy method (based on comparisons with other historical dam failures), empirical formulae, and three independent numerical models. The final width of the breach and the maximum discharge from the breach were estimated using all of these approaches. The aim is to enhance our understanding of the Bílá Desná dam collapse and improve our knowledge of the flood hydrograph and its peak discharge.

2 METHODS

The analysis uses three independent methods, namely historical data analysis, estimation by empirical relationships, and numerical modelling. Particular attention was paid to eliminating the inaccuracies previously reported by Kotaška and Říha (2025). A detailed chronology of critical failure events was established, including the timing of initial leakage, progressive erosion, and final breach formation. The uncertainty in the reservoir volume was explicitly identified as a key factor that influenced the estimates of breach discharge.

The first method estimates the maximum discharge by analogy based on a multiple criteria analysis (MCA) using normalization of criteria with documented embankment dam failures. This involved selecting a set of comparable historical failures based on dam type, height, reservoir capacity, and failure mechanism, normalising them, and then calculating similarity and weight for each selected dam. The final peak flow discharge is calculated by taking the weighted average of the historical discharges.

The second approach used 23 empirical formulae derived from historical dam failure datasets. These formulae were used to estimate critical breach parameters, including breach width, breach formation time, and peak discharge. Empirical relationships offer simplified approximations and are particularly useful when detailed input data is limited. The formulae were applied systematically and the variability among their outputs was analysed to identify a credible range for peak discharge.

The third approach consists of extensive numerical simulations using three independent models:

- AREBA (van Damme et al., 2012), which uses a semi-empirical approach for breach growth and hydrograph estimation;
- DL Breach (Wu, 2016), which applies a physically based erosion model for breach development;
- HEC-RAS 6.6 (Brunner, 2024), a widely used hydraulic modelling tool for simulating unsteady flow and breach evolution.

To address uncertainties in reservoir geometry, two distinct storage–elevation curves were developed:

- based on a Digital Model of Relief (DMR) derived from GIS data (Opendata, 2024), representing current terrain conditions,
- based on historical project documentation (Gebauer, 1916), reflecting the original design geometry.

These curves were used to simulate two breach scenarios, allowing evaluation of how reservoir volume uncertainty influences peak discharge estimates. Each model produced slightly different results, which were compared to establish a credible range for the breach hydrograph.

3 THE BÍLÁ DESNÁ DAM

The breached dam of the Bílá Desná is located in the north of the village of Desná, within the cadastral area of Albrechtice in the Jizera Mountains in Czechia, with coordinates of about 50 ° 48′03″ N, 15 ° 16′37″ E (Fig. 1). The principal objective of the Bílá Desná dam was to stabilize the discharge of local water courses, providing more reliable water use and flood protection. The Bílá Desná basin covers approximately 8.05 km^2 with an average elevation of approximately 800 m above sea level (m a. s. l.).

According to the detailed project (Gebauer, 1916), the Bílá Desná embankment dam was designed with a straight crest 243.5 m long and 4 m wide. The maximum height of the dam was 17.85 m from the foundation and 14 m above the natural ground. The dam was 54 meters wide in the base. The freeboard height was 1.6 m above the maximum water level in the reservoir (818.90 m a. s. l.). The upstream slope was provided with two berms, the lower 1.5 m and the upper 1 m wide. The upstream slope of the dam varied from 1:2 at the toe to 1:1.5 at the dam crest. The slope was protected by a 0.3 cm thick rip-rap made of granite placed on a 0.4 m thick gravel layer. The dam sealing was made of local sandy loam with thicknesses varying between 3 and 5 m. The sealing was terminated in the 4.5 m deep trench and anchored in the subbase by a 2 m deep wood sheet-pile wall. The downstream slope of 1:1.5 was covered with grass.

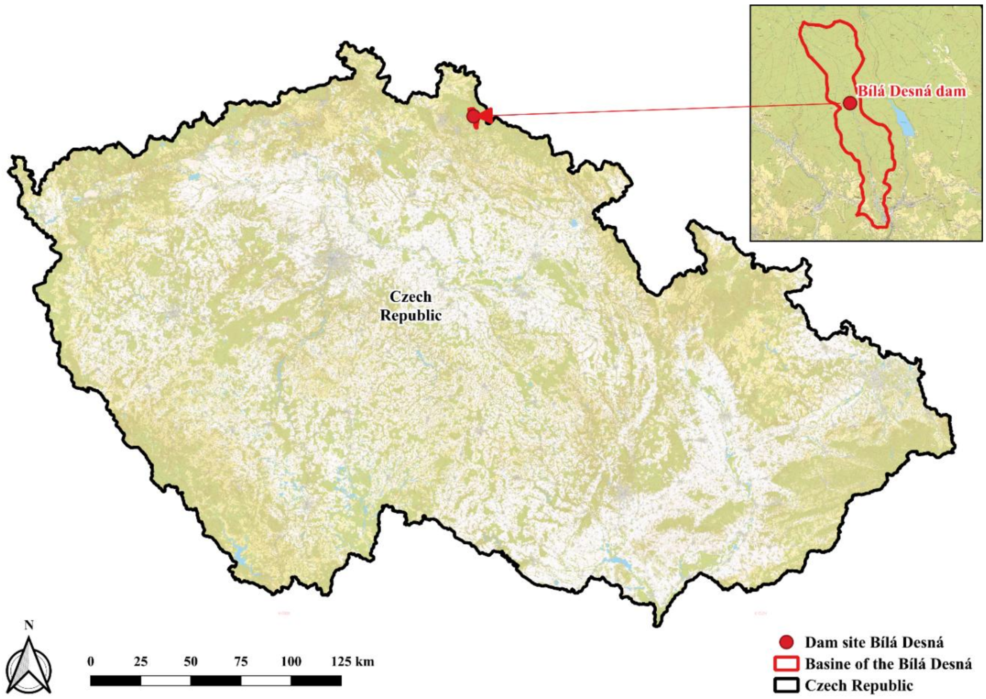

Fig. 1. Location of the Bílá Desná dam site and its catchment area (red polyline).

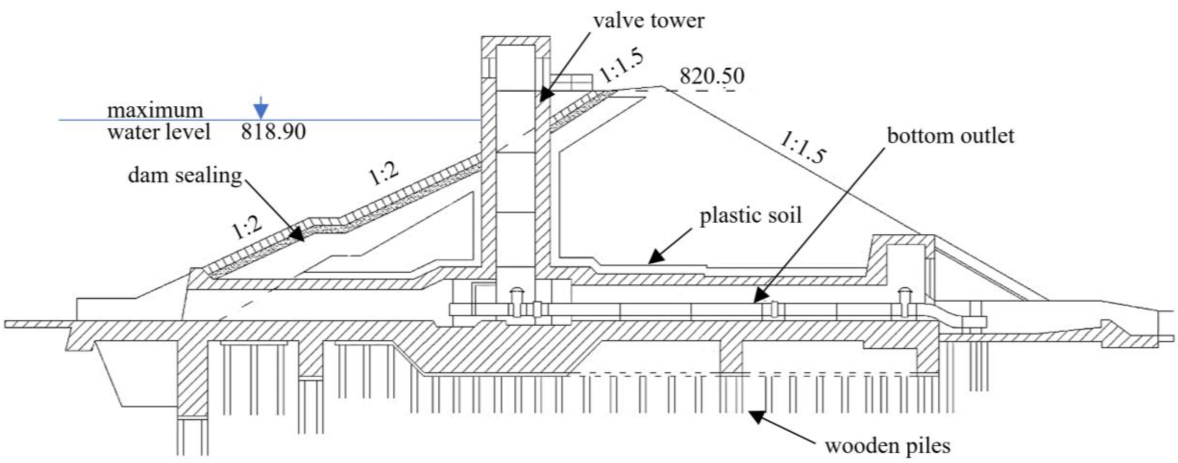

Fig. 2. Dam cross section with outlet gallery and valve tower.

Table 1. Basic parameters of the Bílá Desná dam (Plenkner, 1908; Commission, 1911; Gebauer, 1916; Kotaška and Říha, 2025).

Parameter	Variable	Value	Units
Total reservoir volume	V_{max}	0.400/0.550	[mil. m^3]
Maximum water depth in the reservoir	h_k	12.40	[m]
Lowest bed of the approach channel upstream	H_{CH}	806.50	[m a. s. l.]
Dam crest elevation	C_L	820.50	[m a. s. l.]
Maximum water level in the reservoir	H_k	818.90	[m a. s. l.]
Maximum dam height above the terrain	h_d	14	[m]
Maximum dam height above the foundation joint	h_f	17.85	[m]
Crest width	C_w	4	[m]
Maximum width of the dam at the base	W_{max}	54	[m]
Length of the dam crest	B_R	243.5	[m]
Upstream slope	1:X	1:2, 1:1.5	[V: H]
Downstream slope	1:Y	1:1.5	[V: H]
Capacity of the bottom outlet	Q_o	5.2	[m^3/s]
Level of the axis of the bottom outlet	H_{axe}	807.10	[m a. s. l.]

The bottom outlet was located in the central part of the dam (Figs. 2, 5). It consisted of a 0.8 m diameter pipe equipped with two valves, which could be operated from either the upstream tower or the downstream valve chamber. To prevent water seepage, the gallery of bottom outlets and the tower were covered with plastic soil. The spillway was located at the right abutment. Due to the expected low bearing capacity of the ground, the bottom outlet and spillway were founded on a grate made of wooden piles drilled into the subbase with a span of approximately 1 to 1.25 m. A typical cross section of the dam and bottom outlet is shown in Fig. 2.

The available data on the basic parameters of the Bílá Desná dam are summarized in the Table 1; all altitudes refer to the Adriatic sea water level (the official Austrian datum level at that time).

The volume of the reservoir represented the greatest source of uncertainty. Original documents reported a maximum storage of approximately 400,000 m³ at the highest water level (818.90 m a. s. l.) (Plenkner, 1908; Gebauer, 1920; Gnendiger, 1917; Karpe, 1935), while other sources, including the Commission (1911) and Raška and Emmer (2014), indicated 290,000 m³ at the water level (817.88 m a. s. l.). To address this discrepancy, two storage–elevation curves were developed: the first (Var. 1) based on historical maps and project documentation (Gebauer, 1916), and the second (Var. 2) derived from a digital relief model using GIS (Opendata, 2024). Analysis suggests that at the maximum level (818.90 m a. s. l.), the reservoir volume was approximately 540,000 m³. Both curves are presented in Fig. 3.

Differences in reservoir volumes can be attributed, namely, to the inaccuracy of geodetic methods used at the time of dam construction; some minor differences are due to changes in the terrain relief between the years 1916 and 2024.

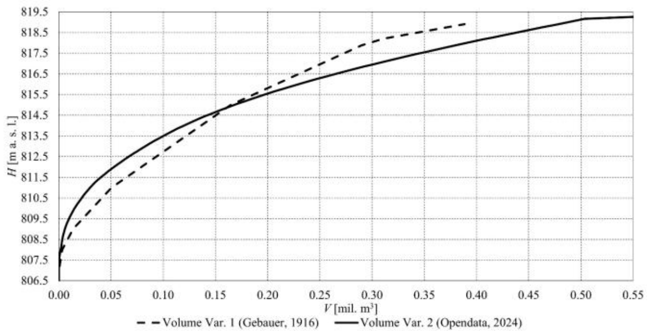

Fig. 3. Storage-elevation curves of the Bílá Desná reservoir according to Gebauer (1916) – Var. 1 and Opendata (2024) – Var. 2.

The dam was proposed as heterogeneous with more permeable downstream shoulder and a layer of clay on the upstream side. Smrček (1917) indicated that the soil was not suitable for the upstream dam sealing, as it contained approximately 85 % of sandy-gravel particles locally containing larger stones, and soils for sealing were similar to those for the shoulder. In the vicinity of the valve tower, the soil was manually tamped.

In 1997, soil samples were taken from the remaining dam body at the right abutment. The soil for the dam (both the sealing and the downstream shoulder) was classified as sandy loam with gravel as SP-SC, SC-SM, or SM according to the Unified Soil Classification System Guide (SML, 1987). The properties of the soil (both sealing and downstream shoulder) are as follows (Smrček, 1917; Žák et al., 2006):

- Percentage of fines < 0.05 mm — 15 %
- Average particle size d_{50} — 0.0023 m
- Cohesion c — 10 kN/m^2
- Dry density of the soil ρ_d — 1850 kg/m^3
- Hydraulic conductivity k — 10^{-6} m/s
- Internal friction angle φ — 38°
- Plasticity index PI — 3 – 4 %
- Porosity n — 0.25

According to Gebauer (1920) and Gnendiger (1917), no extraordinary hydrological conditions, such as floods, were recorded before the dam failure on September 18, 1916. The set of events taken from available sources (Smrček, 1917; Gebauer, 1920; Gnendiger, 1917) are shown in the Table 2.

Table 2. Timing of the failure of Bílá Desná on 18 September 1916 (Smrček, 1917; Gebauer, 1920; Gnendiger, 1917).

Time [hour]	**Time from the first seepage [s]**	**Event description**
15:30	0	No seepage. The reservoir volume about V_0 = 290 000 m^3 at water level H_0 = 817.88 m a. s. l.
15:31	60	The spring of water about 20 mm wide coming from the downstream slope close to the outlet gallery (Fig. 2) at the level H_{pip} = 810.34 m a. s. l.
16:15	2700	Pavement on the upstream slope close to the outlet tower collapsed, a sinkhole occurred. The roof of the breach opening (pipe) collapsed; the soil was quickly washed away.
16:45	4500	The reservoir was completely emptied with the final scour bed at level 806.5 m a. s. l.

The place of an initial seepage on the downstream slope was rather to the left of the gallery portal. The breach developed dominantly on the left side of the bottom outlet, where the piping process was initiated. The progression of erosion towards the right was limited by the gallery; however, it progressed above its roof to the right abutment. The interpretation of the final breach in 1916 was constructed using witnesses' measurements of the final breach opening about one week after the failure (Fig. 4) and with the use of available photographic documentation (Figs. 5, 6).

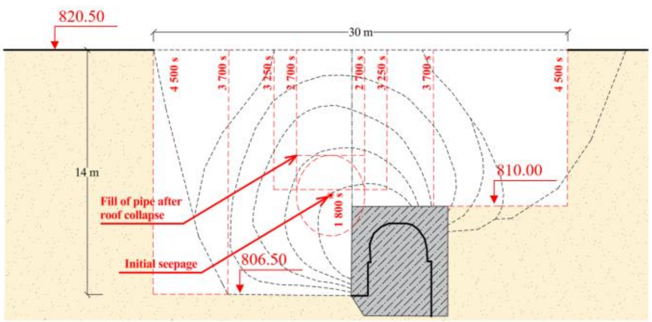

Fig. 4. Interpreted development of the opening of the breach at the axis of a dam (black estimated by Smrček (1917) and red estimated by the authors for Var. 2 at time t = 1800 s, 2700 s, 3250 s, 3600 s, and 4500 s).

The width of the breach at the bottom on the left side of the outlet gallery was approximately 8 m, and the width of the breach opening at the crest of the dam was approximately 32 m. The width at the level of the gallery roof (809.00 m a. s. l.) was about 18 m. From Figs 5 and 6, it can be seen that the breach opening has a funnel shape narrowing towards the flow direction on its sides. This is in agreement with the results of previous experimental studies (Ferguson et al., 2004; Hanson et al., 2005; Alhasan et al., 2015). As the interpretation corresponds to the state about one week after the event, the slopes of the breach probably do not correspond to the shape of the breach during the failure, which tends to be approximately rectangular with vertical sides (Smrček, 1917; Jandora and Říha, 2008).

Fig. 5. View on the breach in the upstream direction, 1916 (Šámalová, 2016).

Fig. 6. View on a cross section of the breach (Šámalová, 2016).

Several internal erosion mechanisms have probably occurred. The percentage of fines indicates susceptibility to internal erosion mechanisms such as segregation, suffusion, contact erosion, or backward erosion resulting in a concentrated leak. The process of arching close to the gallery could cause hydraulic fracturing and thus contribute to the backward erosion piping from the downstream slope. It is probable that during reservoir filling and subsequent 10-month operation, the seepage path developed in the dam body close to the bottom outlet. It is evident that on 8 September 1916, the continuation and progression (Fell and Fry, 2007) of dam failure proceeded quickly.

From a careful analysis, it is clear that the Bílá Desná dam failure mechanism started as backward erosion piping. After the collapse of the erosion pipe roof, the failure proceeded as overtopping. The dam was founded on compressible and permeable subsoil, the foundation of the outlet gallery on the sheet pile frame caused uneven settlement of the embankment, probably resulting in cracks in the bed of the concrete gallery already during construction. Subsequently, minor cracks were observed, even in the concrete of upper part of the gallery (Smrček, 1917).

Based on the maximum water depth in the reservoir (h_k =12.4 m) and the average width of the dam at the base (W_{max} = 54 m), the global critical gradient for Bílá Desná was compared with values reported by various authors (Bligh, 1910; Griffith, 1914; Lane, 1934; Chugaev, 1962; Müller-Kirchenbauer et al., 1993). For the dam configuration and material used (sandy loam), individual authors specified critical global gradients J_{GC} according to Table 3. These gradients were compared to the global critical gradient $J_{C,}$ which stands during the Bílá Desná dam breach (Table 3).

Table 3. Global gradients for sandy loam.

Author	J_{GC}	J_C - Bílá Desná	$J_C \leq J_{GC}$
Bligh (1910)	0.056		No
Griffith (1914)	0.063 to 0.069		No
Lane (1934)	0.118	0.23	No
Chugaev (1962)	0.12		No
Müller-Kirchenbauer et al. (1993)	0.06-0.080		No

The data presented in Table 3 indicate that the seepage lengths, specifically along the foundation and the bottom outlet gallery, were insufficient to prevent backward erosion piping, as they were below the contemporary criteria for internal erosion.

4 REEXAMINATION OF DAM BREAK OUTFLOW

In this chapter, two variants of the Bílá Desná dam breach are simulated using three independent methods and three numerical models based on the reservoir volume storage–elevation curves (Fig. 3) called Var. 1 (Gebauer,1916) and Var. 2 (Opendata, 2024).

4.1 Analogy method

A preliminary idea about peak breach outflow can be obtained by comparing data from real dam failures with characteristics (dam type, height, reservoir volume, breach width) similar to the Bílá Desná dam. From the database (Bernard-Garcia and Mahdi, 2020) on dam failures, 9 "similar" dams were found; their basic characteristics are in the Table 4.

It can be seen that peak discharges for 9 selected dams vary from 110 to 1050 m^3/s. To analyse the peak discharge Q_b, a multiple criteria analysis based on historical dam failures from Table 3 was applied (Hajkowicz and Higgins, 2006). First, the normalization of the criteria (dam height h_d, reservoir volume V_{max}, and breach width B) has been performed.

$$x'_{ij} = \frac{x_{ij} - min(x_j)}{max(x_j) - min(x_j)}\ , \quad j \in \{h_d,\ V_{max}, B\} \tag{1}$$

where i denotes dam No. (Table 4) and x'_{ij} is the normalized value of criterion (j = 1, 2, 3) for dam i = 1, ..., 9. The similarity measure between dam i and estimated dam (D) is the sum of the weighted absolute differences of normalized criteria in the following form:

$$S_i = \sum_j^9 \left| x'_{ij} - x'_{D,j} \right|, \tag{2}$$

Smaller S_i indicates higher similarity. The weight used for the estimate decreases exponentially with smaller similarity. The similarity function of the data set is in the following form:

$$w_i = e^{-pS_i}, \qquad p = 0.25 \tag{3}$$

where p is the decay parameter estimated based on the variability of the data set. Final peak discharge is calculated as similarity-weighted average:

$$Q_b = \frac{\sum_{i=i}^{9} Q_{b,i}\, w_i}{\sum_{i=i}^{9} w_i} \quad (4)$$

Based on results from the Table 4 and Eq. (4), the maximum breach discharge for Bílá Desná was estimated with values of 513 m³/s (Var. 1) and 520 m³/s (Var. 2).

4.2 Empirical Formulae

For a rough estimate of the peak discharge rates, empirical formulae were developed by various authors. Empirical formulae are regression equations based on past dam failure events. However, in general, there is a global shortage of dam-break calibration data due to the scarcity of relevant failure, reliable data from real breached dams are missing, and moreover, data sets are nonhomogeneous because each dam is a unique structure with local hydrological and geological conditions. However, published empirical formulae are often used in dam break analysis to compare real incidents with the results of numerical analysis. Basic parameters of the Bílá Desná dam for an application of empirical equations are listed in Table 6; the equations used are listed in Table 7.

Table 4. Characteristics of 9 similar dams from the database (Bernard-Garcia and Mahdi, 2020) with comparison of the Bílá Desná dam (Gebauer, 1916).

Dam No.	Dam Name	Dam height h_d [m]	Reservoir volume V_{max} [ths. m³]	Breach width B [m]	Peak outflow Q_b [m³/s]
1	Metly	8.5	1930	35	550
2	Bilberry	20	327	37	725
3	Fred Burr	16	750	30	654
4	Ireland Reservoir V.	5.2	160	14	110
5	Kelly Barnes	11.6	777	27	680
6	Laurel Run	13	555	35	1050
7	Lawn Lake	7.9	798	18	510
8	Noppikoski	16.5	1000	42	600
9	Puddingstone	15.2	610	79	480
-	**Bílá Desná**	14	400/550	30	??

Table 5. Results based on Table 4 and equations (1) to (4) according to Var. 1 and Var. 2.

Dam	Normalised dam height h_d	Normalised reservoir volume V_{max}	Normalised breach width B	Similarity measure S_i		Similarity function w_i	
	Var. 1 and 2	Var. 1 and 2	Var. 1 and 2	Var. 1	Var. 2	Var. 1	Var. 2
Metly	0.22	1.00	0.33	1.31	1.23	0.72	0.74
Bilberry	1.00	0.09	0.36	0.55	0.64	0.87	0.85
Fred burr	0.73	0.33	0.25	0.33	0.25	0.92	0.94
Ireland Reservoir V.	0.00	0.00	0.00	0.98	1.07	0.78	0.77
Kelly Barnes	0.43	0.35	0.20	0.43	0.34	0.90	0.92
Laurel Run	0.51	0.22	0.33	0.25	0.16	0.94	0.96
Lawn Lake	0.18	0.36	0.07	0.82	0.73	0.82	0.83
Noppikoski	0.76	0.47	0.44	0.69	0.61	0.84	0.86
Puddingstone	0.68	0.25	1.00	0.95	0.86	0.79	0.81
Bílá Desná	0.59	0.14 0.22	0.25	–	–	–	–

Table 6. Variables used in Equations (5) to (25).

Group	Parameter	Notation	Value	Units
Reservoir characteristic	Dam height above the terrain	h_d	14	[m]
	Length of the dam crest	B_R	243.5	[m]
	Water depth at the beginning of the failure	h_w	11.38	[m]
	Reservoir volume at the beginning of the failure	V_w	290 000 410 000*	[m³]
Breach characteristic	Width of the breach opening at the bottom	b	8	[m]
	Width of the breach opening in the crest	B	30	[m]
	Average breach width	$\bar{B}$	19	[m]
Others	Acceleration due to gravity	g	9.81	[m/s²]
	Discharge coefficient	M	1.0	[m$^{1/2}$/s]

*****Higher values correspond to the reservoir volume in Var. 2 (Fig. 3).

Table 7. Empirical Equations for Estimation of the Peak Discharge.

Author	**Formula for the peak discharge Q_b [m³/s]**	**Eq.**
Soil Conservation Service (1981)	$Q_b = 1.776{V_w}^{0.47}$	(5)
MacDonald and Langridge-Monopolis (1984)	$Q_b = 1.154(V_w h_w)^{0.412}$	(6)
Costa (1985)	$Q_b = 961(V_w/1\cdot 10^6)^{0.48}$ $Q_b = 325(h_w V_w/1\cdot 10^6)^{0.42}$	(7) (8)
Evans (1986)	$Q_b = 0.72{V_w}^{0.53}$	(9)
Costa and Schuster (1987)	$Q_b = 0.0184(V_w h_w \rho g)^{0.42}$	(10)
Molinaro and Maione (1991)	$Q_b = 0.116\left(V_W/{h_w}^3\right)^{0.221} g^{0.5}\, {h_w}^{2.5}$	(11)
Froehlich (1995)	$Q_b = 0.607{V_w}^{0.295}{h_w}^{1.24}$	(12)
Webby (1996)	$Q_b = 0.0443 g^{0.5} V_w^{0.367} h_w^{1.40}$	(13)
Walder and O´Connor (1997)	$Q_b = 1.16{V_w}^{0.46}$ $Q_b = 0.61(V_w h_w)^{0.43}$	(14) (15)
Holomek and Říha (2000)	$Q_b = M\left[b{h_w}^{3/2} + 0.4\dfrac{B-b}{h_w}h_w^{5/2}\right]$	(16)
Jandora and Říha (2008)	$Q_b = 1.6{h_w}^{2.5}$	(17)
Bornschein (2009)	$Q_b = 0.928(h_w V_w)^{0.4319}$	(18)
Xu and Zhang (2009)	$Q_b = \sqrt{g{V_W}^{\frac{5}{3}}}0.133\left(\dfrac{{V_W}^{\frac{1}{3}}}{h_w}\right)^{-1.276} e^{(FM+ER)}$ $FM = -1.232; ER = -1.433$	(19)
Pierce et al. (2010)	$Q_b = 2.325\ln{(h_w)}^{6.405}$ $Q_b = 0.784{h_w}^{2.668}$	(20) (21)
Amini (2011)	$Q_b = 0.6971{V_w}^{0.25}{h_w}^{1.5}$	(22)
Azimi et al. (2015)	$Q_b = 0.453 g^{0.5}{h_w}^{2.5}$	(23)
Tegos et al. (2022)	$Q_b = \mathrm{e}^{(6.09+0.043h_w-0.001\bar{B}+0.0029V_w)}$	(24)
Viard et al. (2022)	$Q_b = ch_d\sqrt{V_r}\,;\quad c = 0.08$	(25)
Kouzehgar and Eslamian (2023)	$Q_b = 21.9522 h_w \bar{B}^{0.4}$ $Q_b = 18.461{h_w}^{1.038}\bar{B}^{0.408}$	(26) (27)

4.3 Numerical modelling

For a more sophisticated and relevant estimate of the outflow hydrograph and peak breach discharge, dam break modelling was carried out using three numerical models. The selection of models was based on the literature review.

4.3.1 Description of the numerical models used

The choice of models was guided by a review of the literature. Simulations were performed using the Rapid Embankment Breach Assessment (AREBA) model (van Damme et al., 2012), DL Breach (Wu, 2016) and HEC-RAS 6.6 with the nonlinear breach growth method (Brunner, 2024). A brief description of the models and their comparison is presented in the following section.

A Rapid Embankment Breach Assessment (AREBA) model was developed by the Flood Risk Management research consortium and universities in England (van Damme et al., 2012). Software enables modelling of the breaching process of an embankment dam due to piping and overtopping. The code was developed using MATLAB software, allowing modifications according to local conditions and the failure mode. A detailed description of the mathematical model is provided by van Damme et al. (2012).

The DL Breach model developed by Wu (2016) is a physically based software to simulate the breaching of embankments due to overtopping or piping. It accounts for noncohesive, cohesive, and composite embankment materials, and represents the growth of the breach by both vertical deepening and lateral widening. The model incorporates reservoir geometry through the storage–elevation relationship and computes breach outflow using hydraulic equations with corrections for submergence effects. Sediment transport is described by non-equilibrium load formulae for noncohesive soils and by headcut erosion processes for cohesive soils. The stability of the breach sidewall and possible collapse are also considered. In piping scenarios, the collapse of the developing pipe roof initiates the transition to overtopping breach. Comprehensive documentation of the model equations can be found in Wu (2016).

DL Breach and AREBA share nearly identical core approaches for simulating homogeneous dam breaches due to internal erosion (piping failure). Both calculate the initial discharge using the same hydraulic principles and use an identical erosion formulation to represent how the breach expands over time and transforms the reservoir. Their differences are subtle and lie mainly in the details of simulating secondary processes, such as the shape of piping breach, losses during breach, how the dam slopes collapse, and how the roof of the piping breach behaves, rather than in their basic hydraulic and erosion formulations (Wu, 2016; van Damme et al., 2012).

In contrast, HEC-RAS (Brunner, 2024) incorporates dam breach modelling within a broader hydraulic simulation framework. It must be noted that the code HEC RAS is not a dam break model, as it preferably serves for flood inundation modelling. The HEC RAS dam break module is simplified, the definition of breach opening and rate of erosion are user specified while DL Breach and AREBA are physically based models. The breach can be defined by entering data directly or using a simplified approach that relates the growth of the breach opening to the flow through the breach. One distinct feature is its nonlinear breach growth method, which was used in this study. Instead of assuming that the breach opening grows at a constant, linear rate from initiation to full formation, it allows the user to define a non-linear growth curve. By entering a series of time intervals and the corresponding breach opening dimensions, the model adjusts the growth rate during the breach formation period. The temporal development of the breach geometry is fully coupled with downstream hydraulic routing in the HEC-RAS framework. Details of the underlying breach modelling approach are provided in Brunner (2024).

To highlight the key characteristics of the selected numerical tools, a comparative overview is presented in the Table 8, which summarizes the type, main assumptions and representation of the breach process, and the typical applicability.

Sensitivity analyses on dam breach models AREBA, DL Breach, and HEC-RAS help to correctly select the parameters that will change during the simulations. A one-way sensitivity analysis conducted by Kotaška (2022) for the AREBA model showed that the Manning roughness and the erodibility coefficient are the parameters that most influence the breach hydrograph, breach size, and failure time. Similarly, the analysis of the DL Breach model by Kotaška and Říha (2022) indicated that the resulting breach discharge and the final width of the breach are highly sensitive to changes in the erodibility and roughness coefficients. Different results were obtained from the HEC-RAS model depending on the method used (Karki et al., 2022). A local sensitivity analysis identified the elevation of the dam breach as the most sensitive parameter for peak outflow. However, a global sensitivity analysis using a Monte Carlo simulation revealed that the most sensitive parameter was the width of the dam breach. Across all three models, understanding and careful definition of critical parameters are essential for reliable dam breach simulations.

4.3.2 Input variables

In dam failure modelling, the following assumptions were taken into account:

- The failure started with a concentrated leakage from an embankment at the level H_0 = 810.34 m a. s. l. (Smrček, 1917; Gebauer, 1920),
- The water level in the reservoir at the beginning of the failure was 817.90 m a. s. l. according to Gebauer (1920),
- The initial water volume in the reservoir differs according to the available data (Fig. 3)
- An initial reported leakage was about 3 l/s (Smrček, 1917), which corresponded approximately with the size of the initial breach opening D_0 = 20 mm.
- The mechanical properties of the soil (percentage of fines, average particle size, cohesion, dry density of the soil, internal friction angle, porosity) were taken from previous investigations and research (Plenkner, 1908; Gebauer, 1916; Smrček, 1917; Žák et al., 2006) and were completed using the available literature (Wahl, 2019) and geotechnical tables (NASEM, 2019) according to the Unified Soil Classification System Guide (SML, 1987).

In the numerical modelling, the aim was to fit the timing of individual recorded events (Table 2) and historical interpretation of the breach development (Fig. 8). It did not include the time of the individual shape of the breach and is rather unreliable as it is more likely imagination about the failure than the real basis for model calibration. The results of the numerical modelling are time-dependent courses of breach parameters such as outflow breach discharge (dam break flood hydrograph), the water level in the reservoir, and the final breach width.

Due to the different computational approaches of the models used, input parameters were divided into two groups. The AREBA and DL Breach models simulate the temporal evolution of the breach based on physical principles. Their calibration involved adjusting the erodibility and Manning roughness coefficients to reproduce the historically documented failure of the Bílá Desná dam. Specifically, the models were calibrated to match the recorded time of roof collapse, the duration of the breaching process, and the final breach geometry (Fig. 4, Table 9).

Table 8. Comparative Characteristics of the Applied Dam Breach Models.

Feature	AREBA	DL Breach	HEC-RAS
Type	Simplified physically-based model	Physically-based numerical model	Comprehensive hydraulic modelling software
Approach	Piping and overtopping failures	Piping and overtopping failures	Piping and overtopping failures
Assumptions	Geometric approximations (circular, rectangular); considers grass cover failure, headcut migration, and empirical roof collapse.	The changing geometry (rectangular pipe, trapezoidal open breach), headcut migration, slope stability of side walls, and mass failure of pipe roof.	User-defined final breach geometry and formation time; breach progression defined by a growth curve (linear/non-linear).
Applicability	Rapid hazard assessment and system-wide risk modelling; optimized for homogeneous embankments.	Physically-based simulation of dam and levee failures (cohesive and non-cohesive materials) in inland and coastal contexts.	Detailed hydraulic modelling of flood routing and inundation mapping based on predefined breach parameters.

Table 9. Input parameters for the physically based models AREBA and DL Breach.

Name of the parameter	Variables	Value	Units
Initial water level in the reservoir	H	817.90	[m a. s. l.]
Initial level of the breach pipe	H_{bp}	810.34	[m a. s. l.]
Initial diameter of the breach pipe	D_0	0.02	[m]
Critical shear stress	τ_c	5	[kPa]
Erodibility coefficient *), **)	k_d	$1.82 \cdot 10^{-5}$	[$m^3/(N.s)$]
Manning´s roughness coefficient *), ***)	n_M	0.025; 0.075	[$s/m^{1/3}$]
Discharge coefficient	M	1	[$m^{1/2}/s$]

*) Subject to model calibration.
**) The erodibility coefficient for overtopping was doubled in the AREBA model.
***) The Manning roughness coefficient was set to 0.025 for DL Breach and 0.075 for AREBA.

Table 10. Peak breach outflows determined by comparison with real failures and using empirical formulae.

<table>
<tr><th colspan="2" rowspan="2">Method</th><th rowspan="2">Eq.</th><th colspan="2">Maximum breach outflow Q_{bmax} [m^3/s]</th></tr>
<tr><th>reservoir volume Var. 1</th><th>reservoir volume Var.2</th></tr>
<tr><td>Analogy method</td><td>multiple criteria analysis</td><td>(1–4)</td><td>513</td><td>520</td></tr>
<tr><td rowspan="27">Empirical formulaes</td><td>Soil Conservation Service (1981)</td><td>(5)</td><td>656</td><td>772</td></tr>
<tr><td>MacDonald, Monopolis (1984)</td><td>(6)</td><td>560</td><td>645</td></tr>
<tr><td rowspan="2">Costa (1985)</td><td>(7)</td><td>530</td><td>626</td></tr>
<tr><td>(8)</td><td>537</td><td>626</td></tr>
<tr><td>Evans (1986)</td><td>(9)</td><td>565</td><td>679</td></tr>
<tr><td>Costa and Schuster (1987)</td><td>(10)</td><td>478</td><td>552</td></tr>
<tr><td>Molinaro and Maione (1991)</td><td>(11)</td><td>510</td><td>551</td></tr>
<tr><td>Froehlich (1995)</td><td>(12)</td><td>359</td><td>508</td></tr>
<tr><td>Webby (1996)</td><td>(13)</td><td>422</td><td>479</td></tr>
<tr><td rowspan="2">Walder and O´Connor (1997)</td><td>(14)</td><td>388</td><td>450</td></tr>
<tr><td>(15)</td><td>378</td><td>443</td></tr>
<tr><td>Holomek and Říha (2000)</td><td>(16)</td><td colspan="2">645</td></tr>
<tr><td>Jandora and Říha (2008)</td><td>(17)</td><td colspan="2">699</td></tr>
<tr><td>Bornschein (2009)</td><td>(18)</td><td>607</td><td>704</td></tr>
<tr><td>Xu and Zhang (2009)</td><td>(19)</td><td>419</td><td>483</td></tr>
<tr><td rowspan="2">Pierce et al. (2010)</td><td>(20)</td><td colspan="2">689</td></tr>
<tr><td>(21)</td><td colspan="2">515</td></tr>
<tr><td>Amini (2011)</td><td>(22)</td><td>621</td><td>677</td></tr>
<tr><td>Azimi et al. (2015)</td><td>(23)</td><td colspan="2">620</td></tr>
<tr><td>Tegos et al. (2022)</td><td>(24)</td><td colspan="2">362</td></tr>
<tr><td>Viard et al. (2022)</td><td>(25)</td><td>490</td><td>583</td></tr>
<tr><td rowspan="2">Kouzehgar and Eslamian (2023)</td><td>(26)</td><td colspan="2">811</td></tr>
<tr><td>(27)</td><td colspan="2">766</td></tr>
</table>

For hydraulics of breach by piping, constant roughness, diameter of the circular opening, and erodibility characteristics were considered along the entire seepage path. For the simulation of an overtopping, the constant discharge coefficient, the roughness of the breach channel, and the erodibility parameters were also constant during the time.

The HEC-RAS code was applied as a simplified parametric model. Since it does not internally simulate physical erosion processes, the known historical data, specifically the failure initiation time, the total failure duration, and the final breach dimensions, were used directly as input parameters (Table 2, Fig. 4). The progression of the breach opening widening and deepening in HEC-RAS was defined by an S-curve to represent the temporal development of the opening.

5 RESULTS AND DISCUSSION

Resulting peak outflows, resp. the outflow hydrographs were determined using the three methods mentioned above, namely the comparison with similar dam failures, empirical formulae, and numerical modelling. Calculations using the latter two methods were carried out for two storage-elevation curves according to Fig. 3. Results coming from the methods described in Sections 4.1 and 4.2 are summarized in the Table 10, where peak breach discharges are compared for the first two methods.

The breach outflow hydrographs and average breach widths obtained from the numerical modelling (Chapter 4.3) were carried out for two variants mentioned above of storage-water stage dependencies according to Fig. 3. Although the peak discharges are relatively similar across the models, the differences in hydrograph shapes reveal variations in how each model handles breach growth and roof collapse.

The initial phase of the hydrographs (t = 0 to 2100 s) is mainly governed by differences in the reservoir volume curves (Fig. 3) rather than by the mechanics of breaching. However, the subsequent difference in hydrograph shapes (Fig. 7) highlights inherent uncertainties in modelling geotechnical instability, despite consistent erosion formulations across the models. While peak discharges align due to dominant hydraulic controls, even in simplified models like HEC-RAS, the distinct algorithms for slope and roof collapse introduce significant variability in the flow profile.

The specific mechanism of roof collapse during piping is the main driver of these shape differences. AREBA employs an empirical prediction method (van Damme et al., 2012), whereas HEC-RAS triggers collapse only when the pipe reaches the dam crest (Brunner, 2024). DL Breach utilizes a physically-based approach where the collapsed roof material is assumed to fall into the pipe space ('virtual space'). This debris must be eroded before expansion continues (Wu, 2016), causing temporary stagnation or decrease in discharge observed around t =3100 s. These discrepancies underscore the necessity of a multi-model approach, as no single formulation can fully capture the complex dynamics of dam failure.

For larger reservoir volume (Var. 2) the hydrographs exhibit higher peak discharges with maximum outflow discharge of about 505 – 520 m^3/s, followed by a rapid decline during reservoir emptying due to a wider opening of the breach (Figs. 7 and 8). The shape of the hydrograph suggests more intensive breaching after the collapse of the "roof" when a larger breach opening develops. Such a high and rapid outflow implies a substantial volume of water being quickly released from the reservoir, probably resulting in documented dramatic consequences downstream of the dam. In the case of a smaller reservoir volume (Var. 1), the discharge increase is less rapid, with a significantly smaller peak discharge of 351 - 359 m^3/s (Fig. 7).

The cross-sectional evolution is detailed in Fig. 4, overlapping the simulated expansion of the breach (using the AREBA model, Var. 2, red lines) with Smrček's historical reconstruction (black lines). The simulation explicitly visualizes the pipe formation and subsequent expansion of the breach after the roof collapse. The discrepancy between the final modelled shape and Smrček's survey can be attributed to the timing of the field data collection, which took place 14 days after failure. During this period, further erosion, weathering, and gravitational slope adjustments inevitably altered the breach geometry compared to the immediate post-flood state.

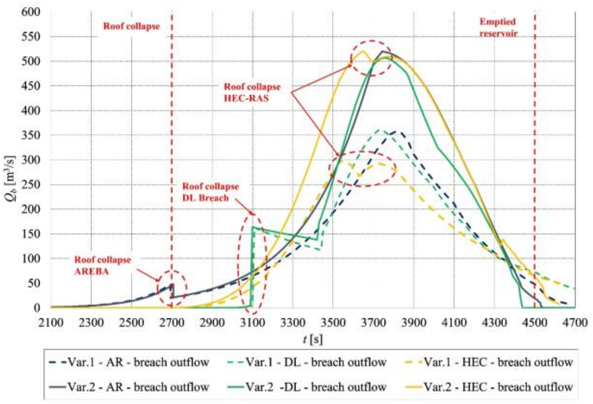

Fig. 7. Results from numerical modelling of the peak discharges and water levels for Var. 1 and Var. 2 (AR - AREBA, DL - DL Breach, HEC - HEC RAS).

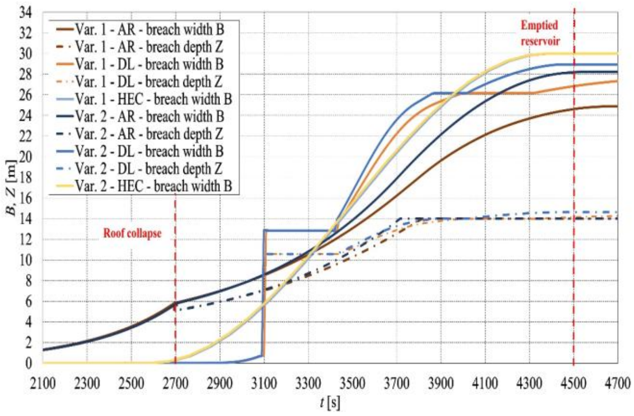

Fig. 8. Results of numerical modelling - breach width (B), breach depth ($Z = C_L – H_b$, where C_L is the dam crest elevation, and H_b is the elevation of the breach bottom) for Var. 1 and Var. 2.

Table 11. Comparison of calculated and documented characteristics of the failure of Bílá Desná.

Variants	Max. breach outflow Q_b [m^3/s]	Maximum breach width B [m]	Time of roof collapse t_p [s]	Reservoir emptying time t_c [s]
AREBA – Var. 1	359	24.9	2692	4688
AREBA – Var. 2	520	28.2	2707	4550
DL Breach – Var. 1	355	27.5	3110	4699
DL Breach – Var. 2	505	28.9	3099	4439
HEC-RAS – Var. 1	351	30	3630	4630
HEC-RAS – Var. 2	518	30	3690	4620
Documented	–	≈30	2700	4500

Table 12. Comparison of calculated and documented characteristics of the Bílá Desná failure by absolute differences of the observed and modelled parameters.

Variants	Maximum breach width ΔB [m]	Time of roof collapse Δt_p [s]	Reservoir emptying time Δt_c [s]
AREBA – Var. 1	5.1	8	188
AREBA – Var. 2	1.8	7	50
DL Breach – Var. 1	2.5	410	199
DL Breach – Var. 2	1.1	399	61
HEC-RAS – Var. 1	0	930	130
HEC-RAS – Var. 2	0	990	120

Table 13. Comparison of the estimated peak breach outflow with other methods and authors.

Author	Breach outflow [m^3/s]	
	Var. 1	Var. 2
Raška and Emmer (2014)	418.2 – 971.8	–
Froehlich (2016); Azimi et al. (2017); Moglen et al. (2019)	320	–
Bernard-Garcia and Mahdi (2020)	320 – 655.6	–
Abdulrahman (2022)	591	–
Analogy method (Section 4.1)	513	520
Empirical formulae (Section 4.2)	359 –811	362 – 811
Numerical modelling AREBA (Section 4.3)	359	520
Numerical modelling DL Breach (Section 4.3)	355	505
Numerical modelling HEC-RAS (Section 4.3)	351	518

Individual numerical models were calibrated by comparing the simulated outputs with the documented failure timeline (Table 2) and the final breach geometry (Fig. 4). The comparison of results from numerical modelling is shown in the Table 11. Fairly good agreement can be seen considering that even documented values may be somewhat uncertain. While the maximum outflow of the breach (Q_b) represents a predicted value due to the absence of historical flow data, the other parameters – maximum breach width (B), roof collapse time (t_p), and reservoir emptying time (t_c) show fairly good agreement with available records, especially considering the inherent uncertainty of the historical documentation.

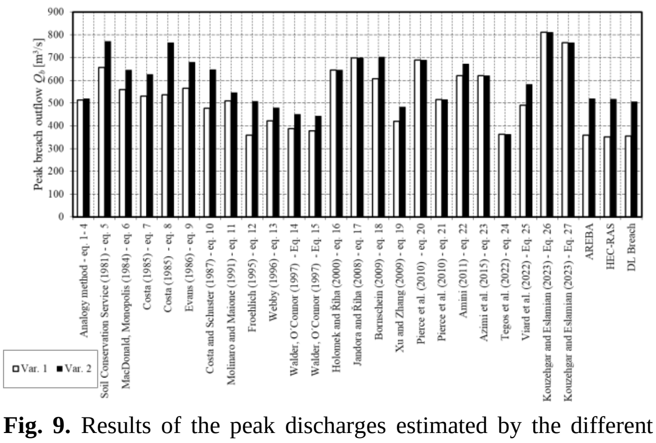

Fig. 9. Results of the peak discharges estimated by the different methods (analogy, empirical formulae, numerical modelling) for Var. 1 and Var. 2.

The "predictive" performance of the numerical models under two variants tested was quantified using the absolute differences of the observed and modelled parameters (maximum width of the breach B, time of roof collapse t_p and reservoir emptying time t_c). As can be seen from Table 12, AREBA software in Var. 2 demonstrates the best agreement with the observed data.

The summary of the results obtained by all methods is shown in a bar graph in Fig. 9. The modelling results fit fairly well with the results obtained by the analogy method and using the empirical formulae. The best fit of the peak breach discharge with the numerical model is provided by the empirical equation (15) of Pierce et al. (2010).

The comparison of the results obtained by individual methods with previously published estimates is shown in the Table 13. In particular, the estimated peak breach outflow from this study falls within the range of values reported by other authors and methods, indicating consistency and alignment with existing literature. The resulting peak breach outflow for the larger reservoir volume (Var. 2) fits better than the one derived for a smaller one (Var. 1). Simplified relations for an estimate of average breach width can be found, e.g., in (Jandora and Říha, 2008) and (Viard et al., 2022). The most probable breach width is between 2 and 4 times the height of the dam ($2h_d$ to $4\ h_d$), with a maximum $5h_d$. In case of the Bílá Desná dam failure, the maximum average breach width is 19 m (Table 6), which is less than $2h_d$ = 28 m. This can be attributed to a relatively narrow valley in the dam profile and the effect of the outlet gallery obstructing the breach opening at its base.

The quantitative assessment highlighted the AREBA model in Var. 2 as the best fit simulation. The validation confirms that the larger reservoir volume assumed in Var. 2 better reflects the historical reality. Based on this validated model, the unknown maximum discharge from the breach is estimated at 520 m^3/s, a value that fits best to the documented timeline and the final geometry of the breach.

6 CONCLUSIONS

This study revisits the Bílá Desná dam failure, the most devastating accident in the history of Czech dams, which occurred in 1916. In the study, available data related to dam design, construction, and operation have been collected and analysed. For the breach outflow estimate, three different methods were used, namely the analogy method, empirical formulae, and numerical modelling with the AREBA, DL Breach, and HEC-RAS software.

The initiating cause of the Bílá Desná dam failure was internal erosion. It was initiated due to a combination of poor dam foundation, poor compaction of the soil in the dam body, poor design with an unacceptably short seepage path, lack of knowledge about the role of filters, and deficiencies in an inlet tower design. After the development and increase of the seepage pipe, the "roof" of the opening collapsed and the failure continued in the overtopping mode.

The backward analysis carried out by three independent methods indicated a peak breach outflow in the range between 359 and 811 m^3/s for Var. 1 (reservoir volume 290 000 m^3 at the failure) and from 362 to 811 m^3/s for Var. 2 (reservoir volume 410 000 m^3). Based on the analysis and incorporating findings from different numerical methods, the peak discharge of the Bílá Desná dam breach is estimated to be approximately 520 m^3/s for Var. 2, predicted with the AREBA model using Opendata (2024), which appears to provide the most realistic hydrograph. The storage-elevation curve in Var. 1 defined by Gebauer (1916) yields a lower value of about 359 m^3/s. These results emphasize the uncertainty in the shape of the breach hydrograph, with various models producing different hydrograph shapes. However, the results of numerical modelling demonstrate strong consistency of the peak breach discharge, the widening of the breach, and the timing of the peak breach discharge of the hydrograph, reinforcing the reliability of the models. These results provide a robust estimate of the maximum flow from the breach and clarify the breach process of the Bílá Desná dam. This was achieved using three independent numerical methods, strengthening the validity and reliability of the findings.

The study demonstrates that when the geometry and hydrograph are constrained by known data, even simplified models such as HEC-RAS may produce reasonable results. However such results and good fit are achieved only when a user can define "known" breach parameters based on data from an incident (such as location of breach opening, time characteristics, geometry and size of final breach opening).

This observation highlights a potential pitfall in validating models solely against well-documented historical failures. High agreement with historical records can be achieved through parameter adjustment (calibration), which may mask underlying structural differences in the models. Therefore, a good fit with past events does not guarantee predictive reliability for future unknown scenarios. True validation requires not only curve fitting, but also rigorous sensitivity analysis and a process-based evaluation of the model's physics.

Acknowledgement: This study is part of the project FAST-S-25-8824 „Optimization of components and appurtenant structures on dams in relation to their safety “.

REFERENCES

Abdulrahman, K., Z., 2022. Peak discharge from breached embankment dams, analysis and prediction. Arabian Journal of Geosciences, 15, 10 p.

Alhasan, Z., Jandora, J., Říha, J., 2015. Study of Dam-break Due to Overtopping of Four Small Dams in the Czech Republic. Acta Universitatis Agriculturae et Silviculturae Mendelianae Brunensis, 63(3), p. 717-729.

Amini, A., B., Nourani, V., Hakimzadeh, H., 2011. Application of Artificial Intelligence tools to Estimate Peak Outflow from Earth DamBreach. International Journal of Earth Sciences and Engineering, 4(6), p. 243–246.

Aureli, Francesca, Maranzoni, Andrea, Petaccia, Gabriella. 2021. Review of Historical Dam-Break Events and Laboratory Tests on Real Topography for the Validation of Numerical Models, Water 13(14), 21/1968 doi: https://doi.org/10.3390/w13141968 https://www.mdpi.com/2073-4441/13/14/1968.

Azimi, R., Vatankhah, A., R., Kouchakzadeh, S., 2015. Predicting peak discharge from breached embankment dams. E-Proc., 36th IAHR World Congress, Hague, Netherlands, 6 p.

Azimi, R., Vatankhah, A., R., Kouchakzadeh, S., 2017. Using Nonlinear Modeling to Predict Peak Discharge and Average Breach Width from Breached Embankment. Azarian J. Agric., 4(5), p. 145-156.

Bernard-Garcia, M., Mahdi, T. F., 2020. A Worldwide Historical Dam Failure's Database. https://doi.org/10.5683/SP2/E7Z09B, Scholars Portal Dataverse, V1.

Bligh, W., G., 1910. Dams. barrages and weirs on porous foundations. Engineering News, 64, p. 708-710.

BMVP. 2025. Breach Model Validation Programme. Internal Erosion Initiated Breach: Model Performance Review & Validation. FWR6124-RT001 R00-00, April 2025, 260 p.

Bornschein, A., 2009. A simple method to estimate inundation due to dam break. Conference: 2nd International Conference of Long Time Behaviour of Dams At: Graz, Austria, 6 p.

Brown, R., J., Rogers, D., C., 1981. BRDAM users' manual. U.S. Department of the Interior, Denver, 67 p.

Brunner, G., W., 2024. HEC-RAS river analysis system: hydraulic reference manual. Version 6.5, Davis, California, 477 p.

Commission, 1911. Fourth report on the activities of the Provincial Commission for the regulation of rivers in the Kingdom of Bohemia for the period 1910–1912, Praha. (in Czech).

Costa, J., E., 1985. Floods from dam failures. Open-File Rep. No. 85-560, USGS, Denver, 54 p.

Costa, J., E., Schuster, R., L., 1987. The formation and failure of natural dams. Open-File Rep. No. 87-392, USGS, Washington, 44 p.

Cristofano, E., A., 1973. Method of Computing Erosion Rate for Failure of Earth fill Dams. United States Department of the Interior, Engineering and Research Center, Denver, CO, No. 727 p.

Davison, M., Hassan, M., Gimeno, O., van Damme, M., 2013. Benchmark study on dam breach and consequence estimation using EMBREA and Life Safety Model. ICOLD Theme C: Computational challenges in Consequence Estimation for Risk Management, p. 241– 254.

Dewals, B., Archambeau, P., Erpicum, S., Mouzelard, T., Pirotton, M., 2002. Coupled computations of highly erosive flows with WOLF software. Proceedings of 5th International Conference on Hydro-Science & Engineering, Warsaw, 10 p.

DHI, 2003. MIKE-11 A modelling system for rivers and channels (manual). Horsholm, Denmark, 510 p.

Evans, S., G., 1986. The maximum discharge of outburst floods caused by the breaching of man-made and natural dams. Canadian Geotechnical Journal, 233, p. 385–387.

Fell, R., Fry, J., J., 2007. Internal Erosion of Dams and their Foundations. Taylor & Francis, New York, 245 p.

Ferguson, K., A., Anderson, S., Sossenkina, E., 2004. Reexamination of the 2004 Failure of Big Bay Dam, Mississippi. In: USSD Annual Conference. San Francisco, California, USA, 34 p.

Fread, D., L., 1984. DAMBRK: The NWS dam break flood forecasting model. National Oceanic and Atmospheric Administration, National Weather Service, Silver Spring, 27 p.

Fread, D., L., 1988a. BREACH An erosion model for earthen dam failures (Model description and user manual). National Oceanic and Atmospheric Administration, National Weather Service, Silver Spring, 35 p.

Fread, D., L., 1988b. The NWS DAMBRK Model: theoretical background/user documentation. National Weather Service, Silver Spring, 315 p.

Froehlich, D., C., 1995. Embankment dam breach parameters revisited. Processed 1995 Conference on Water Resources Engineering, ASCE, New York, p. 887–891.

Froehlich, D., 2016. Predicting Peak Discharge from Gradually Breached Embankment Dam. Journal of Hydrologic Engineering, 15 p.

Gebauer, E., 1916. Project documentation from Ing. Gebauer when the dam is completed with a core and sheet piles, Archive of Povodí Labe.

Gebauer, E., 1920. Zum Dammdurchbruch der Talsperre an der Weissen Desse. B. Förster. Nieder Rochlitz, (in German).

Gnendiger, E., 1917 Der Dammbruch der Talsperre and der Weißen Desse am 18 September des Krieghjahres 1916. Gebrüder Stiepel Ges. Reichenberg, (in German).

Hajkowicz, S., Higgins, A., 2006. A comparison of multiple criteria analysis techniques for water resource management. European Journal of Operational Research, 184, p. 255–265.

Hanson, G., J., Cook, K., R., Hunt, S., L., 2005. Physical modelling of overtopping erosion and breach formation of cohesive embankments. Trans. ASABE, 48(5), p. 1783–1794.

Holomek, P., Říha, J., 2000. A comparsion of breach modelling methods applied to the Slusovice earth dam. Dam Engineering, 93, p. 171-202.

Chugaev, R., R., 1962. Gründungsumriss von Wasserbauwerken. Moskva, Russisa. (In Russian language)

Jandora, J., Říha, J., 2008. The failure of embankment dams due to overtopping. Brno, Czech Republic: Brno University of Technology, 169 p.

Jun, B., Oh, K., 1998. Yeonchun Dam Failure and Downstream Dam-break Flood Analysis. In: Dam Break Modelling, Parallel Session (parallel 43).

Jarrett, R., D., Costa, J., E., 1986. Hydrology, Geomorphology, and Dam-Break Modeling of the July 15, 1982 Lawn Lake Dam and Cascade Lake Dam Failures, Larimer County, Colorado. U.S. Geological Survey Professional Paper 1369. Department Of The Interior, U.S. Geological Survey, 85 p.

Karki, A., Bhattarai, S., Joshi, P., Kafle, M., R., Bhattarai, R., 2022. Dam Breach Analysis and Parameter Sensitivity Analysis Along a River Reach Using HecRas. Stavební obzor - Civil Engineering Journal, 31(4), p. 571–585. doi:10.14311/CEJ.2022.04.0043.

Karpe, L., 1935. Der Dammbruch an der "Weissen Desse" am 18. September 1916. Dominicus Nachf. Teplitz-Schönau, (in German).

Khoshkonesh, A., Nsom, B., Okhravi, S., Dehrashid, F. A., Heidarian, P. DiFrancesco, S. Numerical investigation of dam break flow over erodible beds with diverse substrate level variations. J. Hydrol. Hydromech., Vol. 72, No. 1, 2024, p. 80 - 94.

Kotaška, S., 2022. Sensitivity Analysis of the Software AREBA for Simulation Dam Breaching Due to Internal Erosion. TZB-info (In Czech). [Online] 2022. (last access: 20 March 2025) https://voda.tzb-info.cz/23493-citlivostni-analyza-softwaru-pro-simulace-poruseni-sypanych-hrazi-v-dusledku-vnitrni-eroze

Kotaška, S., Říha, J., 2022. Sensitivity analysis of DL Breach model for simulation Embankment dam breaching due to internal Erosion. 17th international symposium Water management and Hydraulic Engineering (WMHE 2022). Gdańsk: Gdańsk university of technology publishing house, p. 57-58. ISBN: 978-83-7348-874-8.

Kotaška, S., Říha, J., 2025. From Tragedy to Heritage: Retrospective Overview of the Bílá Desná Dam Collapse. International Journal of Architectural Heritage, 19 p. https://doi.org/10.1080/15583058.2025.2558201

Kouzehgar, K., Eslamian, S., 2023. Chapter 2. Application of experimental data and soft computing techniques in determining the outflow and breach characteristics in embankments and landslide dams. In: Handbook of Hydroinformatics, Volume III: Water Data Management Best Practices, p. 11–31.

Lane, E., W., 1934. Security from under-seepage masonry dams on earth foundations. In: Proceedings American Society of Civil Engineers, 60, p. 926-966.

Lumbroso, D., Davison, M., Body, R., Petškovek, G., 2021. Modelling the Brumadinho tailings dam failure, the subsequent loss of life and how it could have been reduced. Natural Hazards and Earth System Sciences, 21 (1), p. 21–37.

MacDonald, T., C., Langridge-Monopolis, J., 1984. Breaching characteristics of dam failures. Journal of Hydraulic Engineering, 1105, p. 567–586.

Moglen, G., E., Hood, K., Hromadka II, T., V., 2019. Examination of Multiple Predictive Approaches for Estimating Dam Breach Peak Discharges. J. Hydrol. Eng., 24(2), 11 p.

Mohamed, A., A., A., Samuels, P., G., Morris, M., W., Ghataora, G., S., 2002. Improving the accuracy of prediction of breach formation through embankment dams and flood embankments. In Proceedings of International Conference on Fluvial Hydraulics, Louvain-la-Neuve, 10 p.

Molinaro, P., Maione, D., 1991. The experience developed by ENEL in dam-break wave computation and flood risk analysis. Colloque International pour la Simulation des Ondes de Submersion, Montréal, Canada.

Morris, M., W., 2011. Breaching of Earth Embankments and Dams. Ph. D. dissertation, Open University, London, 338 p.

Müller-Kirchenbauer, H., Rankl, M., Schlötzer, C. 1993: Mechanism for regressive erosion beneath dams and barrages. In: Brauns, Heibaum and Schuler. Filters in Geotechnical and Hydraulic Engineering. Rotterdam, Balkema, p. 369-376.

NASEM, 2019. Relationship Between Erodibility and Properties of Soils. National Academies of Sciences, Engineering and Medicine Washington. DC: The National Academies Press., 328.

Nogueira, V., D., Q., A., 1988. Mathematical model of progressive earth dam failure. Ph.D. Thesis, Colorado State University, Fort Collins, CO, USA.

Opendata, 2024. Orthophoto. Digital Relief Model 5G. ZM. ZABAGED. https://ags.cuzk.cz/opendata/ (last access: 20 March 2025)

Oguzhan, S., Aksoy, A. O., 2020. Experimental investigation of the effect of vegetation on dam break flood waves. J. Hydrol. Hydromech., Vol. 68, No. 3, 2020, p. 231 - 241.

Petškovek, G., Hassan, M., A., A., M., Lumbroso, D., Collell, M., R., 2020. A Two-Fluid Simulation of Tailings Dam Breaching. Mine Water and the Environment, 40, 151–165 p.

Pierce, M., W., Thornton, C., I., Abt, S., R., 2010. Predicting peak outflow from breached embankment dams. Journal of Hydrology Engineering, 155, 338–349 p.

Plenkner, V., 1908. Projekte der Isertalsperren von W. Plenkner, Sonderabdruck aus der Rundschau für Technik und Wirtschaft, Heft 4.

Rahou, I., Korichi, K., 2023. Comparative analysis of numerical solutions of 2D unsteady dambreak waves using FVM and SPH method. J. Hydrol. Hydromech., Vol. 71, No. 3, 2023, p. 305 - 315.

Raška, P., Emmer, A., 2014. The 1916 catastrophic flood following the Bílá Desná dam failure: The role of historical data sources in the reconstruction of its geomorphologic and landscape effects. Geomorphology, 226, 135–147 p.

Risher, P., Ackerman, C., Morrill-Winter, J., Fields, W., Needham, J., 2017. Levee Breach Consequence Model Validated by Case Study in Joso, Japan, in: X Association of State Dam Safety Conference, 13 p.

Říha, J., Daněček, J., 2000. Mathematical modelling of earth dam breach due to overtopping. Journal of Hydrology and Hydromechanics, 48, 165-179 p.

Singh, V., P., Scarlatos, C., A., 1988. Breach erosion of earthfill dams and flood routing: BEED model. Journal of Natural Hazards, 1, 161-180 p.

SML, 1987. Soil Mechanics Level I, Module 1, Unified Soil Classification System. Study Guide. National Employee Development Staff, Soil Conservation Service, United States Department of Agriculture, 244 p.

Smrček, A., 1917. On the safety of earth dams for water structures and the causes of the catastrophe on the Bílá Desná. Česka matice technicka v Praze, 76 p., (in Czech).

Šámalová, Z., 2016. History of dam construction in the upper Jizera basin. Povodí Labe. a. s. Hradec Králové, 37 p., (in Czech).

Tegos, A., Dooley, B., Dimitriadis, P., Raybould, M., 2022. Predictive empirical dam breach outflows – A global analysis and proposed updates. 21st BDS Conference Dams and Reservoirs in a Climate of Change, 12 p.

Tingsanchali, T., Chinnarasri, C., 2001. Numerical modelling of dam failure due to overtopping. Hydrological Sciences Journal, 46(1), p. 113-130.

Van Damme, M., Morris, M., W., Hassan, M., A., A., M., 2012. A new approach to rapid assessment of breach driven embankment failures. FRMRC II report, 83 p.

Viard, T., Courivaud, J.-R., Laugier, F., Fry, J. J., Squillari, P., 2022. Evaluation of embankment hydraulic structures failure flood wave. Part1: French engineering practices for dam failures. 27th Congrés International CIGB, Marseille, June 2022, Q. 105 – R.19, p. 307 - 347.

Voltz, C., Rousselot, P., Vetsch, D., Faeh, R., 2012. Numerical modelling of non-cohesive embankment breach with the dual-mesh approach. Journal of Hydraulic Research, 2012, 50(6), p. 168-175.

Wahl, T., L., 1998. Prediction of embankment dam breach parameters. Dam Safety Research Report, DSO-98-004, Water Resources Research Laboratory, 67 p.

Wahl, T., L., 2019. Erosion Testing of Zoned Rockfill Embankments. REP. HL-2019-01, U.S. Department of the Interior, Denver, Colorado, USA. 124 p.

Walder, J., S., O´Connor, J., E., 1997. Methods for predicting peak discharge of floods caused by failure of natural and constructed earthen dams. Water Resources Research, 3310, 2337-2348.

Webby, M., G., 1996. Discussion on Peak Outflow from Embankment Dam by Froehlich, 1995a. Journal of water Resources Planning and Management, 1224, p. 316-317.

Wu, W., 2016. Introduction to DLBreach: a simplified physically-based dam/levee breach model, version 2016.4. Technical Report, Department of Civil and Environmental Engineering, Clarkson University, NY, p. 119.

Xu, Y., Zhang, L., M., 2009. Breaching parametrs for earth and rockfill dams. Journal of Geotechnical and Geoenviromental Engineering, 13512, p. 1957-1970.

Zhong, Q., Chen, S., Wang, L., Shan, Y., 2020. Back analysis of breaching process of Baige landslide dam. Landslides, 12 p.

Žák, L., Bláha, J., Jaroušek, J., Charvátová, E., Melanová, M., Rozsypal, A., Simm, O., Vinklát, P., D., 2006. Jizera Mountains dams and the catastrophe on Bílá Desná - a breached dam. Liberec: Desná v Jizerských horách: Knihy 555; Město Desná v Jizerských horách, 155 p., (in Czech).

Received 13 January 2026
Accepted 25 March 2026